Car-Dcros: A Dataset and Benchmark for Enhancing Cardiovascular Artery Segmentation through Disconnected Components Repair and Open Curve Snake

Yuli Wang[1], Wen-Chi Hsu[2], Victoria Shi[3], Gigin Lin[2], Cheng Ting Lin[3], Xue Feng[4], and Harrison Bai[3]

[1] Department of Biomedical Engineering, Johns Hopkins University, Baltimore, MD, 21218, USA
[2] Department of Medical Imaging and Intervention, Chang Gung Memorial Hospital at Linkou, Taoyuan, Taiwan
[3] Department of Radiology and Radiological Science, Johns Hopkins University School of Medicine, Baltimore, MD, 21205, USA
[4] Carina AI, Lexington KY, 40502 USA

Abstract. The segmentation of cardiovascular arteries in 3D medical images holds significant promise for assessing vascular health. Despite the progress in current methodologies, there remain significant challenges, especially in the precise segmentation of smaller vascular structures and those affected by arterial plaque, which often present as disconnected in images. Addressing these issues, we introduce an innovative refinement method that utilizes a data-driven strategy to correct the appearance of disconnected arterial structures. Initially, we create a synthetic dataset designed to mimic the appearance of disconnected cardiovascular structures. Our method then re-frames the segmentation issue as a task of detecting disconnected points, employing a neural network trained to identify points that can link the disconnected components. We further integrate an open curve active contour model, which facilitates the seamless connection of these points while ensuring smoothness. The effectiveness and clinical relevance of our methodology are validated through an application on an actual dataset from a medical institution.

Keywords: Cardiovascular Artery · Segmentation · Disconnected Repairment · Open Curve Snake.

1 Introduction

Cardiovascular diseases rank the highest among the primary causes of mortality and morbidity globally, notably attributable to conditions such as coronary artery disease and stroke [13,6]. Medical imaging techniques, including computed tomography angiography (CTA), enable the visualization of vascular structures. Leveraging 3D vascular structure reconstruction, both topological and morphometric insights can be quantified, facilitating clinical diagnosis and assessment

of vascular health. Such assessments encompass identifying stenosis, plaque formation, occlusions, and more [1,2,11].

A pivotal and intricate phase in vascular structure reconstruction involves precise and automated vessel segmentation. This process entails converting original cardiovascular images into vascular trees with detailed representations of branches, including centerlines and radii. Broadly, two primary methodologies exist for automated vascular tracing. **1) Segmentation-based method**: These techniques segment voxels belonging to the vasculature, followed by vessel skeletonization to identify centerlines iteratively. Subsequently, radii along the centerlines are estimated. In recent years, deep learning approaches, particularly convolutional neural networks (CNNs), have gained prominence in numerous studies for learning robust and discriminative features for automatic vascular segmentation [15,3,9,7,19]. However, current methods such as UNet still encounter challenges in achieving adequate precision, largely due to the small scale and dispersed spatial distribution of cardiovascular structures. Additionally, ensuring the smoothness and continuity of vessels after skeletonization remains uncertain. **2) Tracking-based methods**: These approaches involve the direct identification of initial seeds and radii from seed points, followed by iterative stretching of both ends of the trace during tracking [23,22,17,10]. Crucial to this method is predicting the correct direction for stretching, which can be guided by either a human-designed vessel enhancement filter or a neural network as utilized in CNN Tracker. However, the tracking-based approach is sensitive to the placement of initial seeds. Improper seed selection may lead to tracing leakage into the background or result in an incomplete vascular tree [25].

In our study, we introduce a hybrid refinement methodology that combines segmentation and tracking approaches to achieve robust vessel tracking, leveraging deep learning techniques to enhance cardiovascular artery segmentation through repairing disconnected components and open curve snake methods [18,4]. The primary aim is to rectify disconnected cardiovascular components by accurately identifying the centers of the disconnected parts. The refinement of segmentation by addressing disconnected components has been extensively studied in previous research. For instance, Zhao et al. [27] introduced the Ball B-Spline Curve method for modeling freely shaped tubular objects. Meanwhile, DeepVesselNet [16] specializes in direct vessel segmentation while also focusing on topology and bifurcation detection to minimize disconnected points. However, both approaches require prior knowledge of the locations of disconnected points, which is often unattainable in real clinical settings. Another study, Weng et al. [20,21], proposed a post-processing technique that employs a data-driven approach to mend the topology of disconnected pulmonary tubular structures, training a neural network to predict key points that could connect disjointed components. Yet, its direct tubular connection strategy is unsuitable for cardiovascular arteries. To overcome these challenges in CTA segmentation, we embrace a similar data synthesis and key point detection idea from Weng et al. [20] and advance them by creating a training data synthesis and disconnected connection pipeline in CTA. This pipeline produces disconnected data from complete cardiovascular

trees and improves cardiovascular artery segmentation by repairing disconnected components and utilizing open-curve snake methods.

The key contributions of our work are: 1) Introducing Car-Dcros, a novel pipeline designed to re-frame CTA segmentation by incorporating disconnected component repairment and connection smoothness optimization (open-curve snake) in CTA segmentation. 2) Providing open-source synthetic cardiovascular disconnected datasets specifically tailored for disconnected points detection. 3) Demonstrating state-of-the-art performance on vessel segmentation through benchmarking against three cardiovascular CTA datasets.

2 Methods

In this section, we present a comprehensive description of our approach for detecting disconnected vessel components as a disconnected points detection task. We begin by re-framing the problem and proceed with an explanation of the data synthesis pipeline to create the training dataset. Subsequently, we introduce the revised 3D UNet for objection detection tasks by describing its architecture and implementation details. Finally, we provide a concise overview of the 3D open-curve snake techniques utilized for connecting disconnected points while optimizing for smoothness and density fitness.

2.1 Problem Re-framing

Accurate segmentation of the cardiovascular tree is essential for diagnosing cardiac-related diseases, yet the complexity of cardiac vessel trees, especially with plaque, poses challenges for CNNs to capture fine-grained patterns, often resulting in unsatisfactory predictions and disconnections within vessel tree structures. In this study, we re-frame cardiovascular segmentation as a disconnected points detection and repairment task. Our approach utilizes a neural network to achieve disconnected points detection, a technique commonly applied in computer vision [8,28]. We utilize heatmap regression to create ground-truth heatmaps for each disconnected point. By adopting this, our method produces multi-channel heatmaps, where each channel represents a distinct disconnected point. This technique is particularly effective for identifying the two endpoints of disconnected vessels.

2.2 Data Synthesis Pipline

Due to the absence of public medical datasets for cardiovascular disconnected point detection, we created synthetic data from CTA scans using meticulously annotated vessel masks. This process involved binary mask extraction from 40 the Automated Segmentation of Coronary Arteries (ASOCA) dataset scans [9], 200 the Image Coronary Artery Segmentation (ImageCAS) dataset scans [24], and 10 scans from our dataset (JHH). Our pipeline, illustrated in Fig. 1 (a),

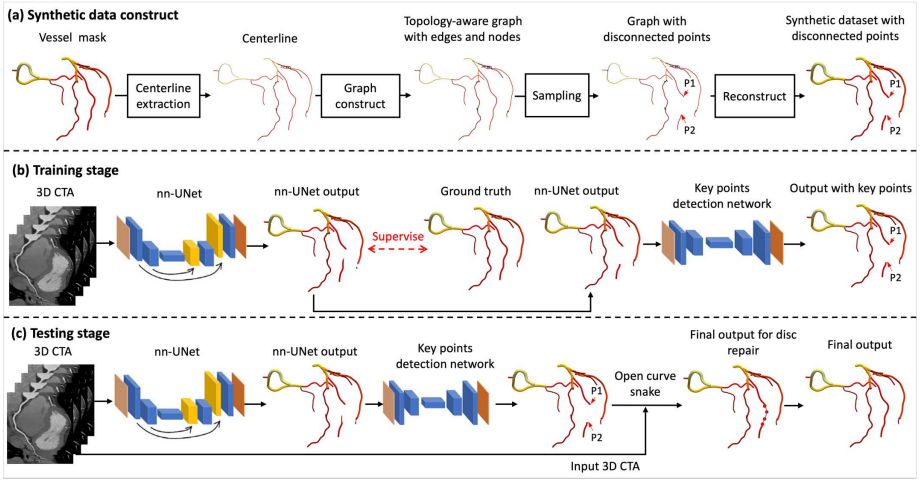

Fig. 1. The pipeline of our framework. (a) In the dataset synthetics, using *ITK* and *Vessel-tree Reconstruction* [26], we identified vessel centerlines and generated tree-like graphs. A branch was randomly chosen, and two points along the centerline were sampled and processed to simulate vascular disconnections, labeled as P_1 and P_2. (b) In training, two networks were trained, including the nn-UNet and the disconnected point detection network. (c) In testing, open curve snake model wass utilized for connecting the disconnected points.

includes centerline extraction, graph construction, random sampling, and reconstruction of disconnected points (P_1 and P_2). To mirror real-world conditions, where discontinuities often occur in thinner vessels, our sampling favored smaller branches by the hierarchy of vessel nodes, leading to discontinuities primarily in smaller vessels.

2.3 Disconnected Point Detection Network

The training pipeline, presented in Fig. 1 (b), encompasses data pre-processing, network architecture, and implementation specifics, all of which are detailed in the following sections.

Data Pre-processing To limit the computing memory, we cropped a sub-volume with the size of 40×40×40 around P_2 where the disconnect occurs and also crop out the disconnected component from the original volume. Specifically, since the location of the small disconnected components P_2 can be found using morphological processes, we randomly selected a point in that small object as the center point of our sub-volume. To keep the same size of the input volume, zero padding was applied to recover the size to 128×128×128.

Details of Network Our network for detecting disconnected points modifies the 3D UNet architecture [5], as shown in Fig. 2. It processes two distinct inputs: the first comprising P_2 and its associated disconnected component, and the second encompassing P_1 and the entire volume. Correspondingly, the network outputs heatmaps for P_1 and P_2. Each input to the network is a binarized subvolume with D, H, and W denoting the spatial dimensions of the cropped volume, 128 in this paper. To preserve coordinate accuracy, we opted to maintain the output heatmaps at the same resolution as the inputs, thereby avoiding downsampling.

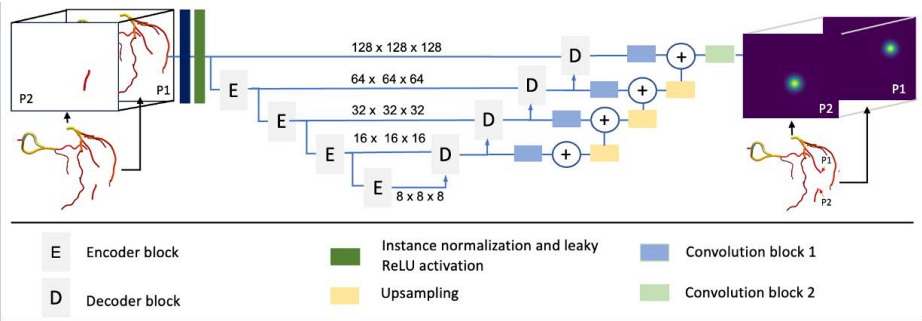

Fig. 2. Detection network for disconnected points: The 3D UNet, receiving two channels representing disconnected components of an artery vessel, processes these inputs and outputs two heatmaps corresponding to points P_1 and P_2.

Implementation Details Our approach involves leveraging an advanced framework for detecting disconnected points, framing the issue as a task of heatmap estimation. The most confident coordinate in each heatmap of H is indicative of the P_{th} disconnected point's position. To create the ground-truth heatmaps, we positioned a 3D Gaussian kernel at the center of each actual disconnected point location. The disconnected point Mean-Squared Error loss is:

$$L = \frac{1}{P}\sum_{p=1}^{P} |H_p - \hat{H}_p|^2, \tag{1}$$

With H_p, $\hat{H}_p$ as the actual and predicted heatmaps for each disconnected point, and P set to 2.

2.4 Model inference with open-curve active contour method

In our model, we connected two identified disconnected points using the open-curve active contour method. Originally developed for 2D image contouring [12], this method refines initial contours iteratively by minimizing an energy function combining external image fitting intensity and internal contour smoothness.

Wang et al. [18] adapted it for 3D neural fibers as an open curve snake, focusing on open curves. The open-curve active contour model used in this paper is a combination of the internal energy E_{int} and the external energy of E_{ext}:

$$E_{total} = \int_0^1 (E_{int}(c(s)) + E_{ext}(c(s)))\ ds, \tag{2}$$

$$E_{int}(c(s)) = \alpha(s)|c_s(s)^2| + \beta(s)|c_{ss}(s)^2|, \tag{3}$$

$$E_{ext}(c(s)) = -I(x(s), y(s), z(s)) + E_{str}(c(s)). \tag{4}$$

However, real scenarios often have unknown locations for disconnected points (P_1 or P_2), and there may be noises scattered throughout the volume's entire original size. We used an algorithm that bridges training with real-world application, improving the prediction of disconnections, as detailed in the Suppl. To reduce the impact of noise scatter, we implemented a noise filter and concentrated on reconnecting the relatively large disconnected components, guided by clinical considerations. Given the minimal clinical impact of small disconnected components on cardiac flow dynamics and plaque detection—due to low signal-to-noise ratios—these small components were excluded from analysis.

3 Experiments

3.1 Datasets

The detailed descriptions of datasets are shown in the Supplementary Material. Two datasets with annotation of arteries are utilized to construct our training dataset. One is the ASOCA dataset which consists of 40 CTA scans and the other one is the ImageCAS dataset with 200 CTA scans. Both datasets are divided into training, validation, and test subsets. The cardiovascular disconnected points synthetic dataset includes 3D models represented by binarized ground-truth segmentation masks, centerlines, disconnected volumes, and a corresponding graphic file for each subject. The graphic file contains information, such as the coordinates, endpoints, and all points along each branch. We also constructed a real-life clinical dataset from the Johns Hopkins Hospital (JHH), consisting of 10 subjects, which is only used for test purposes. The CTA scans from JHH dataset were manually annotated by a senior radiologist.

3.2 Evaluation Metrics

In our experiments, we evaluated the model using the Dice Similarity Coefficient (DSC) and Hausdorff Distance (HD). Both are shown below:

$$\text{DSC} = \frac{2|S \bigcap T|}{|S| + |T|} \qquad \text{HD}(S,T) = \max\left\{\max_{t\in T}\min_{s\in S} d(s,t), \max_{s\in S}\min_{t\in T} d(s,t)\right\} \tag{5}$$

where S and T are the binary labels for both prediction and ground truth, respectively. The DSC values are in the range $[0, 1]$, where 1 indicates perfect overlap between S and T and 0 indicates no overlap. HD measures the proximity between two sets (or segmentations in our instance), with the smaller number indicating better agreement. As is customary we report the 95% HD.

Object Keypoint Similarity (OKS) has been used as the evaluation metric in Weng et al. [20]. In this paper, we adapted OKS to align with the features of our dataset. Our modifications to the OKS are shown below:

$$KS_n = -exp(-d_n^2/2s^2k^2), \qquad OKS_p = \frac{\sum_n KS_n \cdot \delta(v_n > 0)}{\sum_n \delta(v_n > 0)} \tag{6}$$

d_n is the Euclidean distance between actual and predicted disconnected points, with k as the point-specific constant and s the scale of the true object. OKS_p measures the KeyPoint Similarity (KS) for sample n, and V_n is the visibility flag. OKS_p denotes the OKS for each p_{th} point (p=2 in this study), ranging from 0 (no match) to 1 (perfect match).

$$D_d = \frac{1}{P}\sum_{p=1}^{P} |p - \hat{p}| \tag{7}$$

Here D_d is the Euclidean distance between the predicted disconnected point and the ground-truth disconnected point.

4 Results

To analyze the performance of our methods on topology repairing of the disconnected cardiovascular vessels, we used several methods on the proposed dataset, as shown in Table 1 and Table 2.

Table 1. Dice and 95% HD performance on the ASCOS, ImageCAS and JHH dataset

Dataset	Method	Dice	95% HD
ASCOS	nn-UNet (2D)	0.761 ± 0.023	9.32 ± 1.240
	nn-UNet (3D)	0.793 ± 0.031	6.84 ± 1.290
	nn-UNet with clDice	0.801 ± 0.029	2.79 ± 0.945
	nn-UNet with Car-Dcros	**0.845 ± 0.019**	**1.22 ± 0.321**
ImageCAS	nn-UNet (2D)	0.795 ± 0.029	8.62 ± 1.310
	nn-UNet (3D)	0.821 ± 0.022	6.38 ± 1.200
	nn-UNet with clDice	0.828 ± 0.029	2.48 ± 0.679
	nn-UNet with Car-Dcros	**0.862 ± 0.015**	**1.08 ± 0.239**
JHH	nn-UNet (2D)	0.720 ± 0.038	9.89 ± 1.150
	nn-UNet (3D)	0.762 ± 0.029	7.23 ± 1.420
	nn-UNet with clDice	0.779 ± 0.039	3.41 ± 0.813
	nn-UNet with Car-Dcros	**0.821 ± 0.025**	**1.38 ± 0.402**

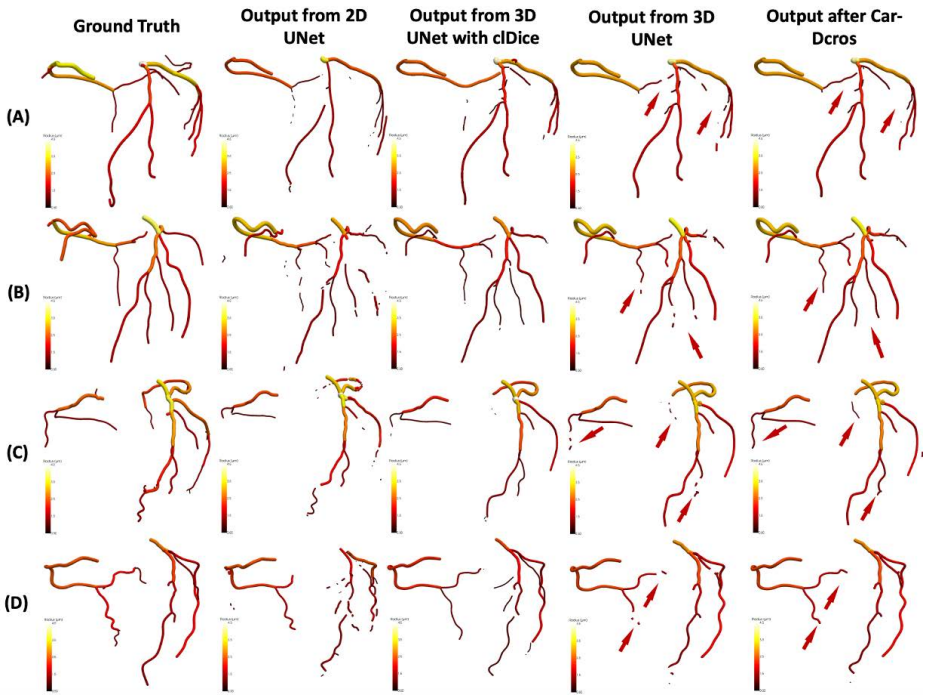

Fig. 3. A qualitative comparison of segmentation results showcases the performance of our proposed models (nn-UNet 3D with Car-Dcros) against various state-of-the-art techniques. Arrows in the results point out the capability of Car-Dcros in correcting disconnections initially identified by the nn-UNet 3D.

Our Car-Dcros model was compared with SOTA methods (2D UNet, 3D UNet, 3D UNet with clDice [14]) across different datasets, as depicted in Fig. 3. We summarized quantitative performance using DSC and 95% Hausdorff Distance metrics in Table 1. UNet with Car-Dcros outperformed others, achieving higher mean DSC and lower mean 95% HD scores, with statistical significance confirmed by a Wilcoxon signed-rank test.

Table 2 presents the performance of disconnected point detection on the ASCOS and ImageCAS datasets. For a detailed assessment, we calculated precision metrics, including overall OKS (mean OKS), OKS^{P1} and OKS^{P2} (OKS for P1 and P2), and mean D_d along with D_d^{P1} and D_d^{P2} for both points. We trained the UNet^1, UNet^2, and UNet^3 networks using synthetic datasets with varying sampled disconnected intervals. Results show that the dual-channel 3D-UNet model is more effective in detecting disconnected points in short, rather than long, vessel intervals. The data also reveals lower average precision for P_1 compared to P_2. This suggests that detecting P_1 is more challenging, likely due to random cropping in data sampling impacting performance, as indicated by poorer D_d and OKS metrics. Additionally, the rarity of disconnected points in smaller cardiovascular arteries makes detecting finer details more difficult.

Table 2. Performance of Disconnected Point Detection. UNet[1]: Input for short disconnections interval (pixel range: 0-5], UNet[2]: Medium disconnections interval (pixel range: 0-10], UNet[3]: Large disconnections interval (pixel range: 0-15].

Dataset	Method	OKS	OKS^{P1}	OKS^{P2}	D_d	D_d^{P1}	D_d^{P2}
ASCOS	**UNet[1]**	**0.769**	**0.765**	**0.878**	**2.83**	**3.31**	**2.37**
	UNet[2]	0.740	0.700	0.838	6.33	7.32	6.10
	UNet[3]	0.692	0.696	0.794	11.61	13.04	9.14
ImageCAS	**UNet[1]**	**0.859**	**0.829**	**0.912**	**2.51**	**3.03**	**2.03**
	UNet[2]	0.823	0.814	0.875	4.22	6.86	4.00
	UNet[3]	0.821	0.804	0.860	10.31	11.94	8.71

5 Conclusion

This research introduces a data-driven refinement technique to overcome the issue of disconnected cardiovascular artery structures, which is vital for accurate diagnosis and effective treatment of cardiovascular diseases. We have developed a method that utilizes a carefully compiled dataset comprising 250 detailed 3D cardiovascular artery structures, in addition to synthetically created disconnected data. Our method involves a neural network specifically tailored to identify points of disconnection. This network is trained with a specialized data synthesis pipeline, which is capable of generating disconnected data from intact cardiovascular artery structures. The outcomes of this method are encouraging, demonstrating a strong potential for application in clinical settings.

Disclosure of Interests. The authors have no competing interests to declare that are relevant to the content of this article.

References

1. Bathina, Y., Bhatia, P.S., Jadiyappa, R.P., Kale, A.: Determining plaque deposits in blood vessels (Oct 11 2016), uS Patent 9,462,987
2. Borkin, M., Gajos, K., Peters, A., Mitsouras, D., Melchionna, S., Rybicki, F., Feldman, C., Pfister, H.: Evaluation of artery visualizations for heart disease diagnosis. IEEE transactions on visualization and computer graphics **17**(12), 2479–2488 (2011)
3. Cao, L., Shi, R., Ge, Y., Xing, L., Zuo, P., Jia, Y., Liu, J., He, Y., Wang, X., Luan, S., et al.: Fully automatic segmentation of type b aortic dissection from cta images enabled by deep learning. European journal of radiology **121**, 108713 (2019)
4. Chen, L., Liu, W., Balu, N., Mossa-Basha, M., Hatsukami, T.S., Hwang, J.N., Yuan, C.: Deep open snake tracker for vessel tracing. In: Medical Image Computing and Computer Assisted Intervention–MICCAI 2021: 24th International Conference, Strasbourg, France, September 27–October 1, 2021, Proceedings, Part VI 24. pp. 579–589. Springer (2021)
5. Çiçek, Ö., Abdulkadir, A., Lienkamp, S.S., Brox, T., Ronneberger, O.: 3d u-net: learning dense volumetric segmentation from sparse annotation. In: Medical Image Computing and Computer-Assisted Intervention–MICCAI 2016: 19th International Conference, Athens, Greece, October 17-21, 2016, Proceedings, Part II 19. pp. 424–432. Springer (2016)
6. Dave, T., Ezhilan, J., Vasnawala, H., Somani, V.: Plaque regression and plaque stabilisation in cardiovascular diseases. Indian journal of endocrinology and metabolism **17**(6), 983 (2013)
7. Dong, C., Xu, S., Dai, D., Zhang, Y., Zhang, C., Li, Z.: A novel multi-attention, multi-scale 3d deep network for coronary artery segmentation. Medical Image Analysis **85**, 102745 (2023)
8. Geng, Z., Sun, K., Xiao, B., Zhang, Z., Wang, J.: Bottom-up human pose estimation via disentangled keypoint regression. In: Proceedings of the IEEE/CVF conference on computer vision and pattern recognition. pp. 14676–14686 (2021)
9. Gharleghi, R., Adikari, D., Ellenberger, K., Ooi, S.Y., Ellis, C., Chen, C.M., Gao, R., He, Y., Hussain, R., Lee, C.Y., et al.: Automated segmentation of normal and diseased coronary arteries–the asoca challenge. Computerized Medical Imaging and Graphics **97**, 102049 (2022)
10. He, H., Banerjee, A., Choudhury, R.P., Grau, V.: Automated coronary vessels segmentation in x-ray angiography using graph attention network. In: International Workshop on Statistical Atlases and Computational Models of the Heart. pp. 209–219. Springer (2023)
11. Jin, Y., Pepe, A., Li, J., Gsaxner, C., Zhao, F.h., Pomykala, K.L., Kleesiek, J., Frangi, A.F., Egger, J.: Ai-based aortic vessel tree segmentation for cardiovascular diseases treatment: status quo. arXiv preprint arXiv:2108.02998 (2021)
12. Kass, M., Witkin, A., Terzopoulos, D.: Snakes: Active contour models. International journal of computer vision **1**(4), 321–331 (1988)
13. Mensah, G.A., Brown, D.W.: An overview of cardiovascular disease burden in the united states. Health affairs **26**(1), 38–48 (2007)
14. Shit, S., Paetzold, J.C., Sekuboyina, A., Ezhov, I., Unger, A., Zhylka, A., Pluim, J.P., Bauer, U., Menze, B.H.: cldice-a novel topology-preserving loss function for tubular structure segmentation. In: Proceedings of the IEEE/CVF Conference on Computer Vision and Pattern Recognition. pp. 16560–16569 (2021)

15. Tan, W., Zhou, L., Li, X., Yang, X., Chen, Y., Yang, J.: Automated vessel segmentation in lung ct and cta images via deep neural networks. Journal of X-ray science and technology **29**(6), 1123–1137 (2021)
16. Tetteh, G., Efremov, V., Forkert, N.D., Schneider, M., Kirschke, J., Weber, B., Zimmer, C., Piraud, M., Menze, B.H.: Deepvesselnet: Vessel segmentation, centerline prediction, and bifurcation detection in 3-d angiographic volumes. Frontiers in Neuroscience **14**, 592352 (2020)
17. Wang, W., Xia, Q., Yan, Z., Hu, Z., Chen, Y., Zheng, W., Wang, X., Nie, S., Metaxas, D., Zhang, S.: Avdnet: Joint coronary artery and vein segmentation with topological consistency. Medical Image Analysis **91**, 102999 (2024)
18. Wang, Y., Narayanaswamy, A., Tsai, C.L., Roysam, B.: A broadly applicable 3-d neuron tracing method based on open-curve snake. Neuroinformatics **9**, 193–217 (2011)
19. Wang, Y., Feng, A., Xue, Y., Shao, M., Blitz, A.M., Luciano, M.D., Carass, A., Prince, J.L.: Investigation of probability maps in deep-learning-based brain ventricle parcellation. In: Medical Imaging 2023: Image Processing. vol. 12464, pp. 578–583. SPIE (2023)
20. Weng, Z., Yang, J., Liu, D., Cai, W.: Topology repairing of disconnected pulmonary airways and vessels: Baselines and a dataset. In: International Conference on Medical Image Computing and Computer-Assisted Intervention. pp. 382–392. Springer (2023)
21. Weng, Z., Yang, J., Liu, D., Cai, W.: Efficient repairing of disconnected pulmonary tree structures via point-based implicit fields. In: Medical Imaging with Deep Learning (2024)
22. Wolterink, J.M., Leiner, T., Išgum, I.: Graph convolutional networks for coronary artery segmentation in cardiac ct angiography. In: Graph Learning in Medical Imaging: First International Workshop, GLMI 2019, Held in Conjunction with MICCAI 2019, Shenzhen, China, October 17, 2019, Proceedings 1. pp. 62–69. Springer (2019)
23. Yang, H., Zhen, X., Chi, Y., Zhang, L., Hua, X.S.: Cpr-gcn: Conditional partial-residual graph convolutional network in automated anatomical labeling of coronary arteries. In: Proceedings of the IEEE/CVF conference on computer vision and pattern recognition. pp. 3803–3811 (2020)
24. Zeng, A., Wu, C., Lin, G., Xie, W., Hong, J., Huang, M., Zhuang, J., Bi, S., Pan, D., Ullah, N., et al.: Imagecas: A large-scale dataset and benchmark for coronary artery segmentation based on computed tomography angiography images. Computerized Medical Imaging and Graphics **109**, 102287 (2023)
25. Zhang, Y., Luo, G., Wang, W., Cao, S., Dong, S., Yu, D., Wang, X., Wang, K.: Ttn: Topological transformer network for automated coronary artery branch labeling in cardiac ct angiography. IEEE Journal of Translational Engineering in Health and Medicine (2023)
26. Zhang, Z., Marin, D., Drangova, M., Boykov, Y.: Confluent vessel trees with accurate bifurcations. In: Proceedings of the IEEE/CVF Conference on Computer Vision and Pattern Recognition. pp. 9573–9582 (2021)
27. Zhao, Y., Wu, Z., Wang, X., Liu, X.: G2 blending ball b-spline curve by b-spline. Proceedings of the ACM on Computer Graphics and Interactive Techniques **6**(1), 1–16 (2023)
28. Zhou, P., Liu, Z., Wu, H., Wang, Y., Lei, Y., Abbaszadeh, S.: Automatically detecting bregma and lambda points in rodent skull anatomy images. PloS one **15**(12), e0244378 (2020)